



Does the apparent diffusion coefficient from diffusion-weighted MRI imaging aid in the characterization of malignant soft tissue tumors and sarcomas

Prajwal Gowda¹ · Gitanjali Bajaj² · Flavio Duarte Silva¹ · Oganesh Ashikyan¹ · Yin Xi¹ · Avneesh Chhabra^{1,3}

Received: 20 October 2022 / Revised: 25 January 2023 / Accepted: 25 January 2023 / Published online: 2 February 2023
© The Author(s), under exclusive licence to International Skeletal Society (ISS) 2023

Abstract

Objective To identify trends in apparent diffusion coefficient (ADC) measurements from diffusion-weighted imaging (DWI) with respect to tumor type classification and other tumor characteristics whether common malignant soft tissue tumors can be distinguished.

Materials and methods A consecutive series of extremity malignant soft tissue tumors and soft tissue sarcomas (STS) among 78 adult patients with conventional MRI and DWI were included. Each case was evaluated with respect to T1/T2 signal alterations and heterogeneity, presence of peritumoral edema, necrosis, cystic changes, internal hemorrhage, and maximum longitudinal dimension blinded to the histology. The ADC mean and minimum were obtained using a free-hand region of interest of the whole tumor and the darkest (lowest signal area) ADC area of the tumor. Kruskal–Wallis and Wilcoxon Rank-Sum Tests were used to determine associations and significance between tumor subtypes. Intraclass correlation (ICC) and kappa calculations were utilized to assess inter-reader agreements for ADC values and reader diagnosis.

Results Liposarcomas showed more heterogeneous T1W images with hyperintense T1W signal when compared to tumors not classified as liposarcoma ($P = 0.046$ and $P = 0.010$, respectively). Liposarcomas were relatively consistent in demonstrating an absence of hemorrhage (81.8%) while undifferentiated pleomorphic sarcomas consistently showed intralesional hemorrhage (90%). When comparing individual tumor classifications against the rest of the samples, lymphomas registered lower mean and minimum ADC values in the whole tumor and in the most hypointense area of the tumor for both readers ($P < 0.05$). The interobserver agreement between the two readers was good to excellent for all four ADC measurements ($ICC = 0.65–0.98$).

Conclusion Diffusion-weighted imaging generated ADC measurements are reproducible but currently offer limited insight in being able to differentiate among different malignant soft tissue tumor and sarcoma histologies. T1W and T2W signal characteristics also offer limited insight in differentiating between soft tissue malignancies.

Keywords Soft tissue sarcoma · Extremity · MRI · DWI · ADC

Introduction

Magnetic resonance (MR) imaging is the primary modality of choice to identify, characterize, and guide the treatment of musculoskeletal soft tissue sarcomas and malignancies [1–4]. A biopsy of the tumor, followed by histological analysis, provides a final diagnosis of soft tissue sarcoma [5]. The utilization of MR imaging to characterize soft tissue tumors has reached the extent of moderate accuracy in differentiating between benign and malignant tumors, as well as various histological grades of tumors [6–8]. There is considerable room for the discovery of techniques

✉ Avneesh Chhabra
avneesh.chhabra@utsouthwestern.edu

¹ Radiology, UT Southwestern Medical Center, Dallas, TX 75022, USA

² Radiology, University of Arkansas Medical School, Little Rock, AR, USA

³ Orthopedic Surgery, UT Southwestern Medical Center, Dallas, TX, USA

that can characterize and differentiate soft tissue sarcomas within the categorization of benign and malignancy. Treatments for different malignant tumors, ranging from liposarcomas to malignant peripheral nerve sheath tumors (MPNST) vary greatly depending on their location and underlying histology [9–11].

Diffusion-weighted imaging (DWI) and derived apparent diffusion coefficient (ADC) mapping are currently utilized to evaluate tumor cellularity in musculoskeletal soft tissue lesions. DWI interrogates free and restricted water diffusion within the tissue of interest. Tumors with lower free water content due to increased cellularity or protein content restrict diffusion [8]. These differences become relevant when comparing different tissue pathologies and their cellular compositions. Furthermore, the degree of diffusion as quantified using ADC mapping has been shown to differentiate between benign and malignant soft tissue tumors [12]. Difficulties in interpreting DWI and ADC measurements may arise due to possible image distortions and artifactual signals in the measurements [13]. However, ADC measurements have been found to be reproducible across readers and among different magnet strengths [8–12]. An analysis of soft tissue sarcomas using ADC measurement for tumor histology diagnosis characterization has not been explored.

We conducted an analysis of histology-proven soft tissue sarcomas blinded to any relevant information apart from their MR imaging findings to identify trends in their ADC

measurements with respect to tumor type classification and other tumor characteristics. Inter-reader reliability analysis was also performed. Our hypothesis was that DWI and ADC measurements offer differentiation and characterization of various common malignant soft tissue tumors and soft tissue sarcomas.

Materials and methods

This study was a cross-sectional retrospective analysis conducted using relevant institutional IRB approval and regulations. Patient informed consent was waived by the institution.

Patient population

An electronic search was conducted across two institutions specifically looking for musculoskeletal extremity contrast-enhanced MR imaging studies performed for soft tissue sarcomas from 2013 to 2021 from PACS (picture archiving and communications system) and sarcoma board lists. Inclusion criteria included both genders, ages between 18 and 100 years old, upper or lower extremity malignant soft tissue sarcomas and tumors, established final histology on biopsy or tumor resection, and a complete series of MR images including T1W, T2W, contrast imaging,

Table 1 Demographics information

Tumor subtype	Sample size (n)
Undifferentiated pleomorphic soft tissue sarcoma	20
Myxofibrosarcoma	13
Synovial sarcoma	12
Liposarcoma	11
Leiomyosarcoma	5
Soft tissue lymphoma	5
Malignant peripheral nerve sheath tumor	4
Histiocytoma	2
Soft tissue chondrosarcoma	2
Spindle cell sarcoma	2
Angiosarcoma	1
Epithelioid sarcoma	1
Patient population	Sample size (mean age \pm SD)
Men	37 (56 \pm 16 years)
Women	41 (53 \pm 17 years)
Tumor location	Sample size (n)
Lower extremity	60
Upper extremity	12
Pelvic wall	5
Chest wall	1

DWI prior to biopsy, and ADC mapping. Exclusion criteria included benign tumors, metastasis, previous surgical resection, or neoadjuvant treatment. Patient demographics included age, gender, and location of the tumor. Retroperitoneal sarcomas and gynecological sarcomas were excluded.

MR imaging

The primary MR imaging modality varied between the different scanners across both institutions (Siemens, GE, and Philips) using institution-based protocols for musculoskeletal tumor imaging. Both 1.5-T scanners and 3-T scanners were used to perform these scans (1.5 T: $n = 49$, 3.0 T = 29). Each imaging series included conventional imaging (T1W, fsT2W), contrast-enhanced imaging (3D volumetric fat-suppressed isotropic voxel, pre- and post-contrast imaging), and DWI/ADC were obtained in all cases as outlined in the inclusion criteria. The parameters were as follows: T1-weighted (repetition time (TR)/echo time (TE), 600–715/9–11 ms; section thickness, 4 mm; axial and sagittal planes), fat-suppressed (fs) T2-weighted (TR/TE, 3600–4500/50–60 ms; section thickness, 4 mm; axial plane), unenhanced and gadolinium-enhanced fsT1W sequence (isotropic resolution, repetition time/echo time (TR/TE), 4.6–6.3/1.4–1.5; section thickness, 1.5 mm isotropic; modified Dixon fat suppression; coronal plane acquisition with axial and sagittal reconstructions; 0.1 mmol/kg gadolinium-based contrast agent). The axial DWI was performed using single-shot echo-planar imaging (TR/TE, 8000–11,700/70–92; section thickness, 4 mm; b values, 50, 400, and 600–800 s/mm² (600 s/mm²: $n = 14$, 800 s/mm² $n = 64$); flip angle, 90°; matrix, 128 × 128; fat suppression, spectral adiabatic inversion recovery; time of acquisition, 5 min 10 s). The ADC value was calculated using all b values, and the ADC map was automatically generated from the scanner.

Data evaluation

Using conventional MR images and DWI, ADC measurements were performed by two readers. These two readers (R1: musculoskeletal fellowship-trained faculty, R2: current musculoskeletal radiology fellow, 6 years post ACGME-equivalent radiology residency training completed internationally) evaluated anonymized MR imaging data sets blinded to the histology-determined diagnosis as well as each other's measurements and diagnosis predictions. Measurement of the maximum longitudinal dimension of the tumor was performed by the first reader, R1. R1 also recorded the tumor signal intensity alterations

and tumor heterogeneity on T1W and fsT2W, intralesional hemorrhage, non-enhancing necrotic-cystic areas, peritumoral edema, post-contrast enhancement, and the maximum longitudinal dimension of the tumor, as mentioned before. Both R1 and R2 measured the mean and minimum ADC values for the entire tumor lesion, as well as for the hypointense area of the lesion on the ADC map. The ADC values were calculated using a free-hand measure of the region of interest. Furthermore, both R1 and R2 attempted to guess the final diagnosis of the lesion based on MR images and DWI.

Statistical analysis

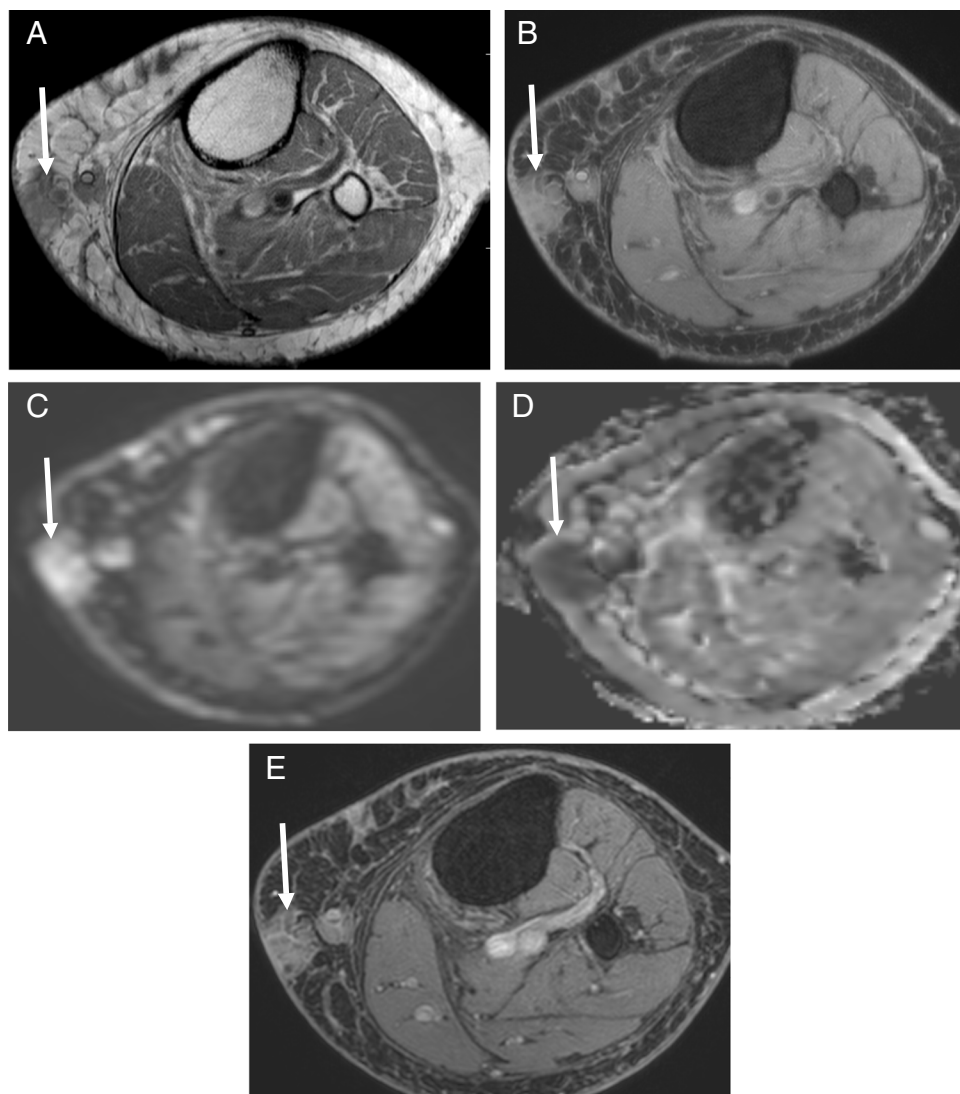
Intraclass correlation (ICC) and kappa calculations were utilized to assess inter-reader agreements between continuous and categorical variables. The continuous variables were the mean and minimum ADC values of the whole tumor and the darkest (most hypointense) area of the tumor, and the categorical variable was the reader diagnosis for determining inter-reader agreements. The agreement was considered poor with ICC/kappa < 0.4; fair, 0.4–0.59; good, 0.6–0.74; and excellent, 0.75–1. Non-parametric Kruskal–Wallis test was used to assess differences in the ADC values between histology-confirmed tumor diagnoses. Non-parametric Wilcoxon rank-sum tests were also conducted between specific histology-confirmed tumor diagnoses and the remaining field of tumors to assess additional differences. Comparisons were made between the sample field as a whole as well as isolating analysis of many of the different tumor types versus the remainder of the field. More specifically, imaging features were also tested between liposarcomas and non-liposarcomas, and between myxoid tumors and non-myxoid tumors. The significance level was set at 0.05. All analyses were done in R 4.0.2 (R core team, Vienna, Austria).

Results

Patient population

In the final inclusion sample, 78 patients with 78 musculoskeletal soft tissue malignancies were included as primary de-novo malignancies. The final diagnoses were determined by surgical histopathology or percutaneous core biopsy. The most common histologies were undifferentiated pleomorphic soft tissue sarcomas, myxofibrosarcomas, and synovial sarcomas, while a few samples were included for other subtypes as well. There was nearly a 1:1 ratio of men to women (47:53). There was only one grade 1 liposarcoma. Other liposarcomas were higher grades (IIs and IIIs) (Table 1).

Fig. 1 A 46-year-old male with medial calf swelling and pain. Proven soft tissue lymphoma. **A** Axial T1W image, **B** axial T2W image of Dixon water map, **C** DWI, **b** = 800 s/mm², **D** ADC map, and **E** post-contrast fsT1W image. Notice mildly heterogeneously enhancing bi-lobed mass (arrows) in the medial subcutaneous tissues with overlying skin thickening. The mean and minimum ADC values of the whole tumor are 0.50 and 0, while the mean and minimum ADC values of the darkest area were 0.25 and 0.20



Conventional MR imaging analysis

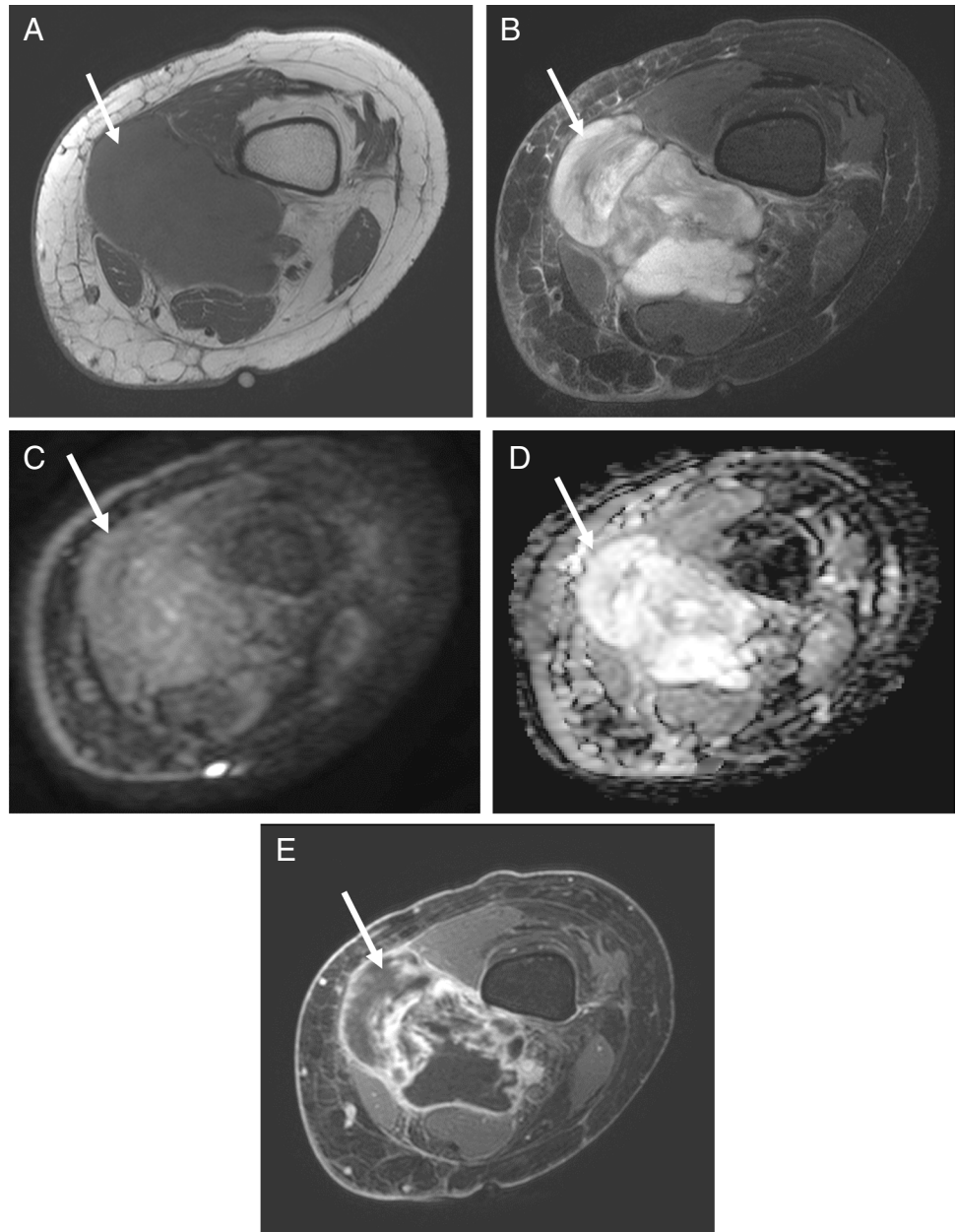
Among different histological tumor grades, the longitudinal tumor dimension was not determined to be significantly different among the 15 sarcoma subtypes ($P = 0.583$), with 1 Burkitt lymphoma registering the largest size (41.6 cm) and one epithelioid sarcoma registering the smallest size (5.6 cm). Among the other categorical signal observations, only T1W signal characteristics and the presence of hemorrhage were determined to be different across the samples ($P = 0.034$ and $P = < 0.001$, respectively). More notably, liposarcomas were relatively consistent in having an absence of hemorrhage (9/11, 81.8%) while undifferentiated pleomorphic sarcomas consistently showed intralesional hemorrhage (18/20, 90%). Liposarcomas were shown to be heterogenous on T1W signal characteristics with a hyperintense T1W signal

when compared to a tumor not classified as a liposarcoma ($P = 0.046$ and $P = 0.010$, respectively). Myxoid tumors were similarly shown to be heterogenous on T2W signal characteristics when compared to non-myxoid tumors ($P = 0.044$).

DWI analysis

Among the 78 malignant soft tissue tumors and sarcomas, the mean ADC value for the whole tumor and the mean ADC value for the darkest region (most hypointense-lowest signal area) of the tumor were determined to be different by both readers (whole tumor: R1 $P = 0.010$, R2 $P = 0.016$; darkest area: R1 $P = 0.021$, R2 $P = 0.011$). A separate analysis was conducted between the three tumor types with the largest sample size (undifferentiated pleomorphic

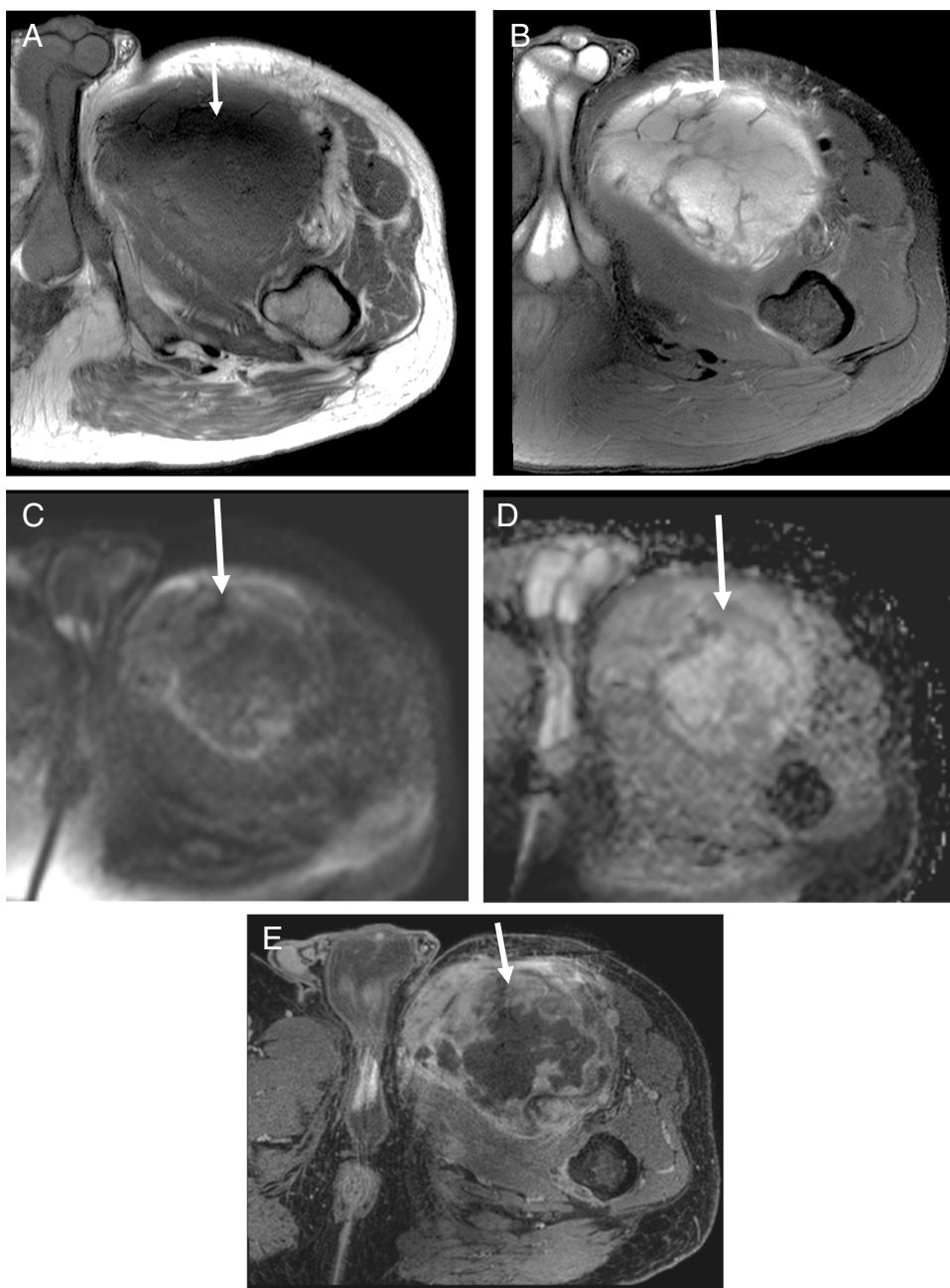
Fig. 2 A 42-year-old female with an undifferentiated pleomorphic soft tissue sarcoma of the left thigh. **A** Axial T1W image, **B** axial T2W image of Dixon water map, **C**, DWI, $b=800$ s/mm², **D** ADC map, and **E** post-contrast fsT1W image. Notice a large heterogeneously enhancing mass (arrows) of the left quadriceps and adductor musculature with cystic/necrotic changes. The mean and minimum ADC values of the whole tumor are 2.50 and 1.50, while the mean and minimum ADC values of the darkest area were 2.10 and 1.65



sarcoma, myxofibrosarcomas, and synovial sarcomas) along with the remaining tumors grouped as a fourth conglomerate. Both readers found a difference in the mean ADC value for the whole tumor between these four groupings ($P < 0.05$). When comparing individual tumor classifications against the rest of the samples, lymphomas registered lower ADC values in all four dependent, continuous variables for both readers ($P < 0.05$). Consistently lower ADC values were demonstrated when comparing synovial sarcomas to the

remainder of the sample, but only with respect to the mean ADC value of the whole tumor ($P < 0.05$ for R1 and R2). Both readers found significant differences in ADC values when differentiating between liposarcomas and non-liposarcomas when analyzing the whole tumor ADC mean, darkest area ADC mean, and darkest area ADC minimum ($P < 0.05$ for R1 and R2). Both readers found significant differences in ADC values when differentiating between synovial sarcomas and non-synovial sarcomas with respect to the

Fig. 3 A 52-year-old male with a myxofibrosarcoma of the left femur. **A** Axial T1W image, **B** Axial T2W image of Dixon water map, **C** DWI, $b = 800$ s/mm², **D** ADC Map, and **E** post-contrast fsT1W image. Notice a large heterogeneously and peripherally enhancing mass (arrows) of the left quadriceps musculature with myxoid changes. The mean and minimum ADC values of the whole tumor are 1.85 and 0.30, while the mean and minimum ADC values of the darkest area were 0.90 and 0.65



minimum ADC value of the whole tumor ($P < 0.05$ for R1 and R2). Notable cases are displayed in Figs. 1, 2, 3 and 4, and full statistics are available in Tables 2, 3, 4, and 5.

Inter-reader analysis

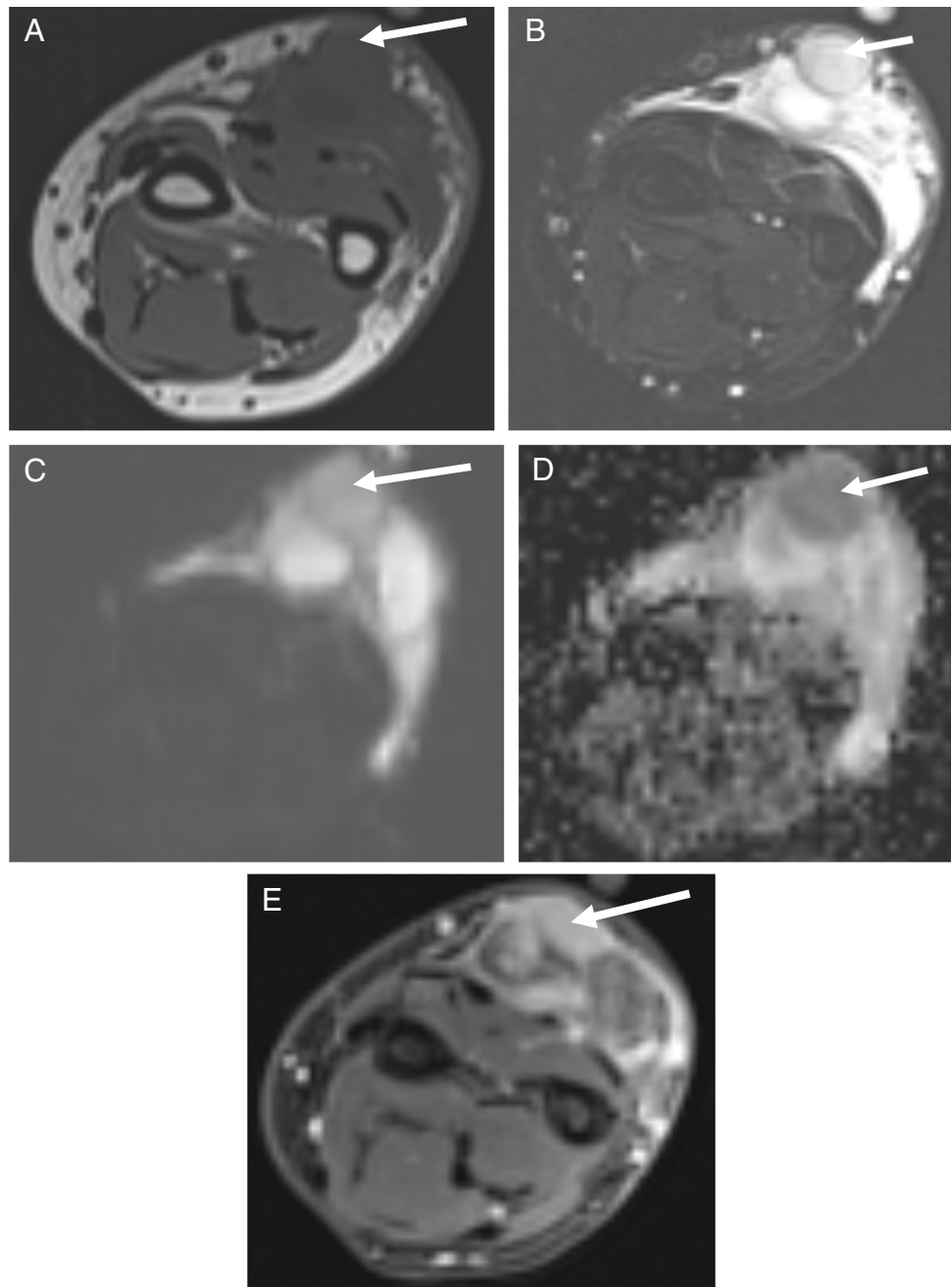
The interobserver agreement between the two readers was good to excellent for all four continuous measurements (ADC values) ($ICC = 0.65–0.98$). The interobserver agreement between the two readers was poor with respect

to arriving at the same diagnosis given the same case ($ICC = 0.31$). Figure 5 displays a Bland–Altman plot of mean ADC values of the whole tumor compared between the two readers.

Discussion

This study provides insight into the utility of DWI and its associated ADC values in differentiating among various malignant soft tissue tumors and sarcoma histologies using MRI. While we generally did not find systematic ADC

Fig. 4 A 38-year-old female with a high-grade liposarcoma of the extensor compartment of the right forearm. **A** Axial T1W image, **B** axial fsT2W image, **C** DWI, $b = 800 \text{ s/mm}^2$, **D** ADC map, and **E** post-contrast fsT1W image. Notice a large heterogeneously enhancing mass (arrows) of the right forearm subcutaneous tissues with heterogeneity and areas of increased T1W signal alteration. The mean and minimum ADC values of the whole tumor are 1.80 and 0.385, while the mean and minimum ADC values of the darkest area were 1.25 and 1.20



differences among various soft tissue malignancies and though limited in scope, there was a demonstrated difference in ADC values of the whole tumor and the darkest (most hypointense/lower signal) area across a wide array of soft tissue sarcoma subtypes by both readers ($P < 0.05$). Calculating a similar value when reducing the number of classifications of tumors further validated that utilizing the mean ADC value for the whole tumor shows differences between a few histological classifications. More interestingly, mean ADC values for the whole tumor were consistently lower for synovial sarcomas and lymphomas when compared to other soft tissue sarcomas. Utilizing

circumstantial factors, such as age and tumor location, may enhance the utility of the ADC values to instantly provide a more plausible diagnosis of the tumor before histology can confirm the diagnosis. Using ADC, authors have been able to differentiate grade I from grade III sarcomas but not grade I from grade II [8]. This study focused on the unique aim of differentiating among various soft tissue malignancies without significant success. The work suggests the limited capability of DWI for histologic characterization apart from a few select tumors with packed cellularity, e.g., round cell tumors like lymphoma or synovial sarcomas. Ahlawat et al. demonstrated the utility of DWI

Table 2 Apparent diffusion coefficient measurements: all tumors

Variables	N (%)	Whole tumor ADC mean (mean ± SD)		Whole tumor ADC minimum (mean ± SD)		Darkest area ADC mean (mean ± SD)		Darkest area ADC minimum (mean ± SD)	
		R1	R2	R1	R2	R1	R2	R1	R2
		Angiosarcoma	1 (1.3%)	1.3 ± NA	1.2 ± NA	0.4 ± NA	0.3 ± NA	0.7 ± NA	0.8 ± NA
B-Cell Lymphoma	3 (3.8%)	0.7 ± 0.2	0.8 ± 0.2	0.2 ± 0.2	0.1 ± 0.2	0.7 ± 0.1	0.6 ± 0.2	0.3 ± 0.3	0.5 ± 0.1
Burkitt's Lymphoma	1 (1.3%)	0.6 ± NA	0.4 ± NA	0.0 ± NA	0.0 ± NA	0.3 ± NA	0.2 ± NA	0.2 ± NA	0.0 ± NA
Chondrosarcoma	2 (2.6%)	1.4 ± 0.4	1.4 ± 0.4	0.3 ± 0.4	0.3 ± 0.4	0.7 ± 0.5	0.7 ± 0.1	0.4 ± 0.6	0.5 ± 0.3
Epithelioid Sarcoma	1 (1.3%)	1.0 ± NA	1.1 ± NA	0.6 ± NA	1.3 ± NA	0.9 ± NA	0.8 ± NA	0.8 ± NA	0.6 ± NA
Fibrosarcoma	1 (1.3%)	1.2 ± NA	1.1 ± NA	0.0 ± NA	0.0 ± NA	0.7 ± NA	0.8 ± NA	0.6 ± NA	0.7 ± NA
Histiocytoma	2 (2.6%)	1.7 ± 0.4	1.7 ± 1.1	0.0 ± 0.0	0.3 ± 0.1	1.2 ± 0.8	1.1 ± 0.6	0.9 ± 0.4	1.0 ± 0.6
Leiomyosarcoma	5 (6.4%)	1.2 ± 0.2	1.2 ± 0.2	0.2 ± 0.2	0.4 ± 0.3	0.9 ± 0.1	0.9 ± 0.2	0.7 ± 0.3	0.7 ± 0.2
Liposarcoma	11 (14.1%)	1.7 ± 0.6	1.6 ± 0.6	0.3 ± 0.7	0.7 ± 0.7	1.5 ± 0.6	1.4 ± 0.6	1.1 ± 0.7	1.3 ± 0.6
MPNST	4 (5.1%)	1.7 ± 0.5	1.7 ± 0.6	1.0 ± 0.4	0.9 ± 0.3	1.1 ± 0.3	1.1 ± 0.3	0.9 ± 0.3	0.9 ± 0.3
Myxofibrosarcoma	12 (15.4%)	1.7 ± 0.5	1.7 ± 0.5	0.5 ± 0.5	0.7 ± 0.5	1.2 ± 0.5	1.3 ± 0.4	1.0 ± 0.6	1.2 ± 0.4
Pleomorphic Sarcoma	20 (25.6%)	1.5 ± 0.4	1.5 ± 0.4	0.4 ± 0.5	0.5 ± 0.5	1.0 ± 0.4	0.8 ± 0.4	0.8 ± 0.4	0.7 ± 0.4
Spindle Cell Sarcoma	2 (2.6%)	1.4 ± 0.5	1.4 ± 0.4	0.5 ± 0.7	0.5 ± 0.3	1.1 ± 0.2	1.1 ± 0.4	0.9 ± 0.4	0.9 ± 0.4
Synovial Sarcoma	12 (15.4%)	1.1 ± 0.3	1.1 ± 0.3	0.2 ± 0.2	0.3 ± 0.2	0.8 ± 0.2	0.8 ± 0.2	0.6 ± 0.2	0.7 ± 0.2
T-Cell Lymphoma	1 (1.3%)	0.6 ± NA	0.6 ± NA	0.1 ± NA	0.2 ± NA	0.5 ± NA	0.5 ± NA	0.5 ± NA	0.5 ± NA
P-Value (Kruskal–Wallis)		0.01	0.02	0.23	0.31	0.02	0.01	0.16	0.01

Table 3 Apparent diffusion coefficient measurements: liposarcomas vs. non-liposarcomas

Variables	N (%)	Whole tumor ADC mean (mean ± SD)		Whole tumor ADC minimum (mean ± SD)		Darkest area ADC mean (mean ± SD)		Darkest area ADC minimum (mean ± SD)	
		R1	R2	R1	R2	R1	R2	R1	R2
		Liposarcomas	67 (85.9%)	1.4 ± 0.5	1.4 ± 0.5	0.4 ± 0.4	0.5 ± 0.4	1.0 ± 0.4	0.9 ± 0.4
Non-Liposarcomas	11 (14.1%)	1.7 ± 0.6	1.6 ± 0.6	0.3 ± 0.7	0.7 ± 0.7	1.5 ± 0.6	1.4 ± 0.6	1.1 ± 0.7	1.3 ± 0.6
P-value (Wilcoxon rank sum test)		0.03	0.04	0.17	0.53	<0.01	0.01	0.02	<0.01

Table 4 Apparent diffusion coefficient measurements: myxoid vs. non-myxoid

Variables	N (%)	Whole tumor ADC mean (mean ± SD)		Whole tumor ADC minimum (mean ± SD)		Darkest area ADC mean (mean ± SD)		Darkest area ADC minimum (mean ± SD)	
		R1	R2	R1	R2	R1	R2	R1	R2
		Myxoid tumors	66 (84.6%)	1.4 ± 0.5	1.4 ± 0.5	0.3 ± 0.4	0.5 ± 0.4	1.0 ± 0.4	0.9 ± 0.4
Non-myxoid tumors	12 (15.4%)	1.7 ± 0.5	1.7 ± 0.5	0.5 ± 0.5	0.7 ± 0.4	1.2 ± 0.5	1.3 ± 0.4	1.0 ± 0.6	1.2 ± 0.4
P-value (Wilcoxon rank sum test)		0.03	0.06	0.10	0.08	0.07	<0.01	0.35	<0.01

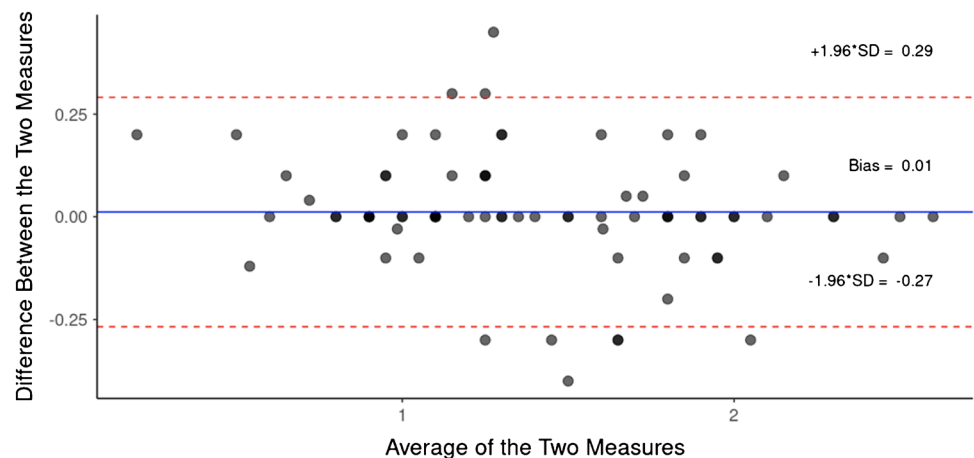
in benign vs. malignant tumors, and Demehri et al. showed the utility of ADC in benign versus malignant peripheral nerve sheath tumors [12–14]. Our results are similar to previously reported works of Ashikyan et al. and Santos et al. using limited sample sizes and expand to the body of knowledge in this domain [15, 16]. Ashikyan et al. had

also reported a minimum ADC of 0.8, and the mean ADC was 1.2 among a case series of synovial sarcomas.

The other notable finding of this study was the good to the excellent agreement seen in ADC values ($ICC = 0.65–0.98$), but poor agreement in diagnosis prediction by the two readers ($ICC = 0.31$). This implies

Table 5 Apparent diffusion coefficient measurements: synovial vs. non-synovial

Variables	N (%)	Whole tumor ADC mean (mean ± SD)		Whole tumor ADC minimum (mean ± SD)		Darkest area ADC mean (mean ± SD)		Darkest area ADC minimum (mean ± SD)	
		R1	R2	R1	R2	R1	R2	R1	R2
		Synovial tumors	66 (84.6%)	1.1 ± 0.3	1.1 ± 0.3	0.2 ± 0.2	0.3 ± 0.2	0.8 ± 0.2	0.8 ± 0.2
Non-synovial tumors	12 (15.4%)	1.5 ± 0.5	1.5 ± 0.5	0.4 ± 0.5	0.5 ± 0.4	1.1 ± 0.5	1.0 ± 0.5	0.8 ± 0.5	0.9 ± 0.5
P-value (Wilcoxon rank sum test)		0.57	<0.01	<0.01	0.02	0.09	0.04	0.12	0.04

Fig. 5 Bland Altman plot of mean ADC values of the whole tumor when comparing the two readers' measurements

that while multiple readers can accurately measure ADC values within a reasonable margin of error, the image alone may lend itself to widely varying interpretations and diagnosis. Myxoid soft tissue malignancies tend to exhibit higher mean ADC. The minimum ADC for myxofibrosarcomas in our study was 0.5–1.2. Although minimum ADC values were variable among different sarcomas (0.0–1.3), these were again found to be the lowest for lymphoma.

This study has a few limitations. First, soft tissue sarcomas and malignancies are uncommon, and many are diagnosed on histology before MRI with DWI is obtained. As a result, numerous tumor categorizations hold only one or a few cases, which limited the interpretation of the Kruskal–Wallis test. To minimize the impact, analyses were performed with clinically meaningful dichotomizations of the subtypes. Second, only a few centers routinely do DWI. Thus, different magnets are commonly used for their imaging. It is hoped that in the future, a multi-center effort can lead to the collation of a larger sample of cases with more uniform imaging and produce new knowledge in this domain.

In conclusion, diffusion-weighted imaging and apparent diffusion coefficient currently offer limited insight in being

able to differentiate among soft tissue malignant tumors and sarcomas while preserving good to excellent inter-reader agreement in measurements. T1W and T2W signal characteristics also offer limited insight in differentiating between soft tissue malignancies.

Declarations

Conflict of interest AC receives royalties from Jaypee and Wolters. AC also serves as a consultant with ICON Medical and Treace Medical Concepts, Inc. AC is a speaker for Siemens. AC is a medical advisor and has a research grant from Image biopsy lab Inc. The authors do not report any conflict of interest.

References

- Murphey MD, Kransdorf MJ, Smith SE. Imaging of soft tissue neoplasms in the adult: malignant tumors. *Semin Musculoskelet Radiol.* 1999;3(1):39–58.
- Kransdorf MJ, Bancroft LW, Peterson JJ, Murphey MD, Foster WC, Temple HT. Imaging of fatty tumors: distinction of lipoma and well-differentiated liposarcoma. *Radiology.* 2002;224(1):99–104.

3. Murphey MD, Gibson MS, Jennings BT, Crespo-Rodríguez AM, Fanburg-Smith J, Gajewski DA. From the archives of the AFIP: imaging of synovial sarcoma with radiologic-pathologic correlation. *Radiographics*. 2006;26(5):1543–65.
4. Walker L, Thompson D, Easton D, Ponder B, Ponder M, Frayling I, et al. A prospective study of neurofibromatosis type 1 cancer incidence in the UK. *Br J Cancer*. 2006;95(2):233–8.
5. Coran A, Ortolan P, Attar S, Alberioli E, Perissinotto E, Tosi AL, et al. Magnetic resonance imaging assessment of lipomatous soft-tissue tumors. *In Vivo*. 2017;31(3):387–95.
6. Gielen JL, De Schepper AM, Vanhoenacker F, Parizel PM, Wang XL, Sciort R, et al. Accuracy of MRI in characterization of soft tissue tumors and tumor-like lesions. A prospective study in 548 patients. *Eur Radiol*. 2004;14(12):2320–30.
7. Berquist TH, Ehman RL, King BF, Hodgman CG, Ilstrup DM. Value of MR imaging in differentiating benign from malignant soft-tissue masses: study of 95 lesions. *AJR Am J Roentgenol*. 1990;155(6):1251–5.
8. Chhabra A, Ashikyan O, Slepicka C, Dettori N, Hwang H, Callan A, et al. Conventional MR and diffusion-weighted imaging of musculoskeletal soft tissue malignancy: correlation with histologic grading. *Eur Radiol*. 2019;29(8):4485–94.
9. Vanhoenacker FM, Van Looveren K, Trap K, Desimpelaere J, Wouters K, Van Dyck P, et al. Grading and characterization of soft tissue tumors on magnetic resonance imaging: the value of an expert second opinion report. *Insights Imaging*. 2012;3(2):131–8.
10. Mesko NW, Wilson RJ, Lawrenz JM, Mathieu JL, Ghiam MK, Mathis SL, et al. Pre-operative evaluation prior to soft tissue sarcoma excision - why can't we get it right. *Eur J Surg Oncol*. 2018;44(2):243–50.
11. Dyrop HB, Vedsted P, Rædkjær M, Safwat A, Keller J. Imaging investigations before referral to a sarcoma center delay the final diagnosis of musculoskeletal sarcoma. *Acta Orthop*. 2017;88(2):211–6.
12. Ahlawat S, Khandheria P, Subhawong TK, Fayad LM. Differentiation of benign and malignant skeletal lesions with quantitative diffusion weighted MRI at 3T. *Eur J Radiol*. 2015;84(6):1091–7.
13. Fisher S, Wadhwa V, Manthuruthil C, Cheng J, Chhabra A. Clinical impact of magnetic resonance neurography in patients with brachial plexus neuropathies. *Br J Radiol*. 2016;89(1067):20160503.
14. Demehri S, Belzberg A, Blakeley J, Fayad LM. Conventional and functional MR imaging of peripheral nerve sheath tumors: initial experience. *AJNR Am J Neuroradiol*. 2014;35(8):1615–20.
15. Ashikyan O, Bradshaw SB, Dettori NJ, Hwang H, Chhabra A. Conventional and advanced MR imaging insights of synovial sarcoma. *Clin Imaging*. 2021;76:149–55.
16. Santos FS, Verma N, Marchiori E, Watte G, Medeiros TM, Mohammed TH, et al. MRI-based differentiation between lymphoma and sarcoidosis in mediastinal lymph nodes. *J Bras Pneumol*. 2021;47(2):e20200055.

Publisher's note Springer Nature remains neutral with regard to jurisdictional claims in published maps and institutional affiliations.

Springer Nature or its licensor (e.g. a society or other partner) holds exclusive rights to this article under a publishing agreement with the author(s) or other rightsholder(s); author self-archiving of the accepted manuscript version of this article is solely governed by the terms of such publishing agreement and applicable law.